

## Optical conductivity of superconducting $\text{Sr}_2\text{RuO}_4$

BALÁZS DÓRA<sup>1</sup>, KAZUMI MAKI<sup>2</sup> and ATTILA VIROSZTEK<sup>3,4</sup>

<sup>1</sup> *The Abdus Salam ICTP, Strada Costiera 11, Trieste, I-34014, Italy*

<sup>2</sup> *Department of Physics and Astronomy, University of Southern California, Los Angeles CA 90089-0484, USA*

<sup>3</sup> *Department of Physics, Budapest University of Technology and Economics, H-1521 Budapest, Hungary*

<sup>4</sup> *Research Institute for Solid State Physics and Optics, P.O.Box 49, H-1525 Budapest, Hungary*

PACS. 74.70.Pq – Ruthenates.

PACS. 74.25.Gz – Optical properties.

PACS. 74.20.Rp – Pairing symmetries (other than s-wave).

**Abstract.** – We compute the optical conductivity of 2D f-wave superconductors and also of the multigap model proposed recently by Zhitomirsky and Rice at  $T = 0\text{K}$  in the Born limit. The presence of interband impurity scattering was found to play an important role: the contributions from the two bands mix up, and new structures are seen in the tunneling density of states and in the optical spectrum as well, corresponding to interband transitions. This will provide a sensitive test in selecting the competing models for the triplet superconductivity in  $\text{Sr}_2\text{RuO}_4$ .

*Introduction.* – The discovery of superconductivity in  $\text{Sr}_2\text{RuO}_4$  in 1994 has generated much interest since it is a perovskite with the same crystal structure as  $\text{La}_2\text{CuO}_4$  [1]. From analogy with superfluid  $^3\text{He}$  Rice and Sigrist [2,3] proposed the spin triplet p-wave superconductor with order parameter

$$\Delta(\mathbf{k}) = \mathbf{d}\Delta_p(T)(\hat{k}_x \pm i\hat{k}_y) \quad (1)$$

Here  $\mathbf{d}$  is the spin vector parallel to  $z$ .

The triplet pairing has been confirmed by the presence of spontaneous magnetization seen by  $\mu\text{SR}$  [4], which revealed that the superconducting state breaks the time-reversal symmetry, and a flat  $^{17}\text{O}$  Knight shift seen by NMR [5] showed no change in the spin susceptibility when passing through the superconducting transition temperature. However the large density of states ( $N(0)$ ) in the gapless region was somewhat surprising [6], since eq. (1) has the full energy gap [7].

Furthermore, as sample quality improved, the characteristics of nodal superconductors became clearly visible in the specific heat ( $\propto T^2$ ) [8], the magnetic penetration depth ( $\propto T^2$ ) [9], NMR relaxation rate ( $\propto T^3$ ) [10], the thermal conductivity ( $\propto T^2$ ) [11,12] and the ultrasonic attenuation [13]. Therefore a variety of 2D f-wave models have been proposed

[14, 15, 16]. Since all these f-wave models have the same quasiparticle density of states, the specific heat and the magnetic penetration depth etc. are described equally well by any of these 2D f-wave models [16]. On the other hand, the angular dependent magnetothermal conductivity data by Izawa et al. [17] can exclude all 2D f-wave models with nodes lying in the  $a - b$  plane [16, 18].

Therefore it singles out the most consistent f-wave as

$$\Delta(\mathbf{k}) = \mathbf{d}\Delta_f(T)(\hat{k}_x \pm i\hat{k}_y) \cos(ck_z). \quad (2)$$

The nodal lines are horizontal. Also the pair correlation takes the maximum value for the relative separation of the pair at  $\pm c$ . However in quasi-two dimensional systems with paramagnon (i.e. the ferromagnetic fluctuation), the ground state of p-wave superconductors is given by eq. (1) [3]. This is why Zhitomirsky and Rice (ZR) [19] proposed the multigap model: there is p-wave superconductor attached the active  $\gamma$  band, which induces another f-wave like order parameter in the passive  $\alpha + \beta$  bands through Cooper pair scattering given by

$$\Delta_2(\mathbf{k}) = \mathbf{d}\Delta_2(T)(\hat{k}_x \pm i\hat{k}_y) \cos(ck_z/2). \quad (3)$$

Since  $\Delta_2(\mathbf{k})$  as given in eq. 3 gives the same quasiparticle density of states as a d-wave superconductor [20], it is not difficult to reproduce the specific heat and the magnetic penetration depth within the multigap model as was shown recently by Kusunose and Sigrist [21].

However a simple analysis suggests that  $\Delta_2(\mathbf{k})$  is incompatible with the angular dependent magnetothermal conductivity data. In fig. (1) we show  $\Delta(\mathbf{k})$  for p-wave, f-wave and  $\Delta_2(\mathbf{k})$  in quasi 2D systems.

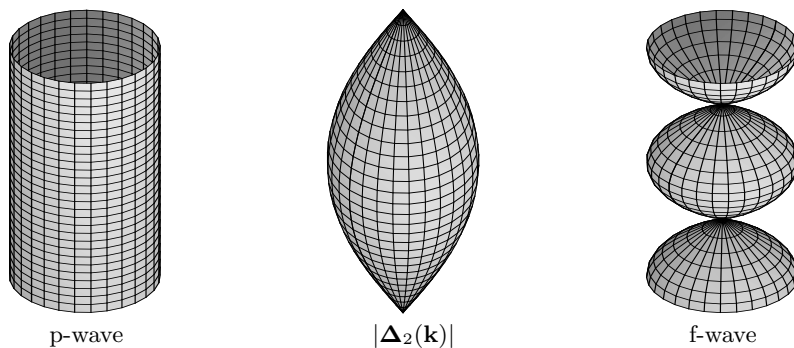


Fig. 1 – The absolute value of the p-wave (left),  $\Delta_2(\mathbf{k})$  (middle) and f-wave gap is shown. Note the presence of horizontal nodes in the latter two.

We note here that  $\mathbf{v}_c = 0$  (i.e. the Fermi velocity in the  $z$  direction) on the nodal lines of  $\Delta_2(\mathbf{k})$  which gives rise to a large  $\cos(2\phi)$  term in the angular dependent thermal conductivity [16].

In the following we compute the quasiparticle density of states and the optical conductivity for the f-wave gap and for the multigap model in the Born limit at  $T = 0\text{K}$ , assuming, that both inter- and intraband scattering of impurities are important, which was predicted to have strong effect on the superconducting state [22]. The density of states differs significantly in these two models, producing distinct peaks from the active and passive bands in the ZR model, while only one single peak is found in the f-wave case. In the optical conductivity, beyond the intraband resonance peaks another extra feature is found coming from interband scattering. On the other hand, the single broad bump in the f-wave case can clearly be distinguished from

the three peak structure of ZR's model, hence both the single particle density of states and the optical conductivity manifest evident signatures of the corresponding model.

*Density of states.* – As already pointed out by Agterberg [22], the effect of interband impurity scattering plays an important role in the multigap model, similarly to the interband scattering of Cooper pairs, which induced  $\Delta_2(\mathbf{k})$  in the passive bands. However, in the f-wave case, we deal with a simple one band model, therefore only intraband impurity scattering is considered.

The effect of weak impurities (Born limit) is incorporated in the quasiparticle Green's function of the multigap model by renormalizing the frequency:

$$\Delta_2 u_1 = \omega + \Gamma_{11} \frac{2}{\pi} \frac{u_1}{\sqrt{1-u_1^2}} K\left(\frac{1}{\sqrt{1-u_1^2}}\right) + \Gamma_{12} \frac{u_2}{\sqrt{1-u_2^2}}, \quad (4)$$

$$\Delta_p u_2 = \omega + \Gamma_{21} \frac{2}{\pi} \frac{u_1}{\sqrt{1-u_1^2}} K\left(\frac{1}{\sqrt{1-u_1^2}}\right) + \Gamma_{22} \frac{u_2}{\sqrt{1-u_2^2}}, \quad (5)$$

where  $u_1$  and  $u_2$  are the dimensionless frequencies renormalized by  $\Delta_2$  and  $\Delta_p$  in the passive ( $\Delta_2$ ) and active ( $\Delta_p$ ) channels, respectively,  $\Gamma_{jl} = n_i \pi N_l |U_{jl}|^2$  ( $j, l = 1, 2$ ), where the total density of states is split as  $N_1 : N_2 = 0.43 : 0.57$  between the passive  $\alpha + \beta$  and the active  $\gamma$  bands from de Haas-van Alphen measurement [23].  $U_{11}$  and  $U_{22}$  are the intraband,  $U_{12} = U_{21}$  are the interband scattering matrix elements,  $n_i$  is the impurity concentration,  $K(z)$  is the complete elliptic integral of the first kind. As opposed to this, for the f-wave model, the frequency is renormalized as

$$\frac{\omega}{\Delta_f} = u - \frac{\Gamma}{\Delta_f} \frac{2}{\pi} \frac{u}{\sqrt{1-u^2}} K\left(\frac{1}{\sqrt{1-u^2}}\right), \quad (6)$$

where  $\Gamma = n_i \pi N_0 |U|^2$ ,  $N_0 = N_1 + N_2$  is the total density of states. At the Fermi energy ( $\omega = 0$ ), the frequencies are obtained as

$$u_1 = 4i \exp\left(\frac{\pi}{2} \Delta_2 \frac{\Delta_p - \Gamma_{22}}{\Gamma_{11}(\Delta_p - \Gamma_{22}) + \Gamma_{12}\Gamma_{21}}\right), \quad (7a)$$

$$u_2 = \frac{\Delta_2}{\Delta_p} \frac{\Gamma_{21}}{\Gamma_{11}(1 - \Gamma_{22}) + \Gamma_{12}\Gamma_{21}} u_1, \quad (7b)$$

$$u = 4i \exp\left(\frac{\pi \Delta_f}{2\Gamma}\right) \quad (7c)$$

for small  $\Gamma$ 's. The quasiparticle density of states (DOS) is obtained as

$$N_{\text{multigap}}(\omega) = \text{Im} \left( N_1 \frac{u_1}{\sqrt{1-u_1^2}} K\left(\frac{1}{\sqrt{1-u_1^2}}\right) + N_2 \frac{u_2}{\sqrt{1-u_2^2}} \right), \quad (8)$$

$$N_f(\omega) = N_0 \text{Im} \frac{u_1}{\sqrt{1-u_1^2}} K\left(\frac{1}{\sqrt{1-u_1^2}}\right) \quad (9)$$

for the multigap and f-wave model, respectively. In the Born limit, the importance of interband scattering readily follows from eq. (7). Without interband processes, the two bands decouple, and the p-wave gap behaves like an s-wave gap in the presence of nonmagnetic impurities: it remains gapped for small impurity concentrations, and reaches the gapless region only for

high concentrations or strong scatterers. In the density of states, peaks are expected at the gap maxima of the two bands, namely at  $\omega = \Delta_2$  and  $\Delta_p$ . As soon as interband scattering is present, the p-wave channel becomes gapless for arbitrary concentration and strength, as is seen from eq. 7. In figs. 2 and 3, the density of states is plotted for  $U_{11} = U_{22} = U$ ,  $\Gamma = 0.001\Delta_p$  and for weak ( $\Gamma_{12}N_0/N_2 = 0.0001\Delta_p$ ) and strong ( $\Gamma_{12}N_0/N_2 = 0.1\Delta_p$ ) interband scattering. Here we used  $\Delta_2 = 0.3\Delta_p$  following refs. [19, 21], which was found to describe very well the experimentally obtained specific heat and penetration depth. Also for the f-wave model, the weak-coupling relation  $\Delta_f = 1.21\Delta_p$  was assumed. In the weak interband scattering limit, the DOS in the  $\gamma$  band increases very slowly, while for strong impurities, even a small peak develops at  $\omega = \Delta_2$  in the p-wave DOS, due to the strong interplay of the two bands. For the f-wave model, only one peak is present at  $\omega = \Delta_f$ , henceforth clear indications of either the multigap or the f-wave model should be observed experimentally.

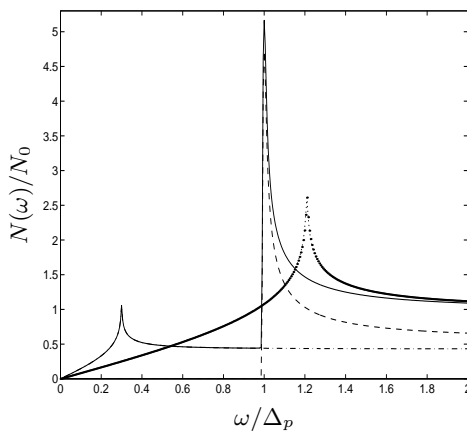


Fig. 2

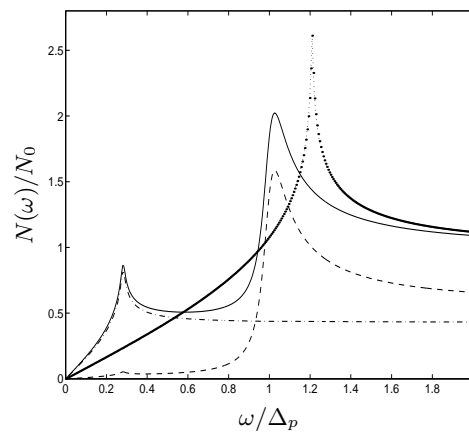


Fig. 3

Fig. 2 – The density of states is shown for weak interband scattering for the multigap model: in the passive band (dashed-dotted line), active band (dashed line) and the full DOS (solid line). The corresponding f-wave DOS (dotted line) exhibits one single peak at  $\omega = 1.21\Delta_p$ .

Fig. 3 – The density of states is plotted for strong interband scattering. The peak in the p-wave channel (dashed line) at  $\omega = 0.3\Delta_p$  indicates the influence of these kind of processes.

In fig. 4, the DOS is shown for medium strength inter- and intraband scatterers:  $U_{jl} = U$ ,  $\Gamma = 0.1\Delta_p$ . The peaks at the gap maxima are broadened into big bumps and increasing density of states is observable in the p-wave channel below the gap maximum. In fig. 5, the DOS of both models are compared, as intraband scattering increases.

*Optical conductivity.* – In the following we consider the optical conductivity of the multigap and f-wave model at  $T = 0\text{K}$ . In the former case, as a lowest order approximation, each band contributes separately to the optical response, which is obtained as

$$\text{Re}\sigma(\omega) = \zeta_1 \text{Re}\sigma_1(\omega) + \zeta_2 \text{Re}\sigma_2(\omega), \quad (10)$$

where  $\zeta_1 = (n_1/m_1)/(n/m) = 0.64$ ,  $\zeta_2 = (n_2/m_2)/(n/m) = 0.36$ , which measures the contribution of each band to the conductivity [23]. At  $T = 0\text{K}$ , the conductivities are obtained

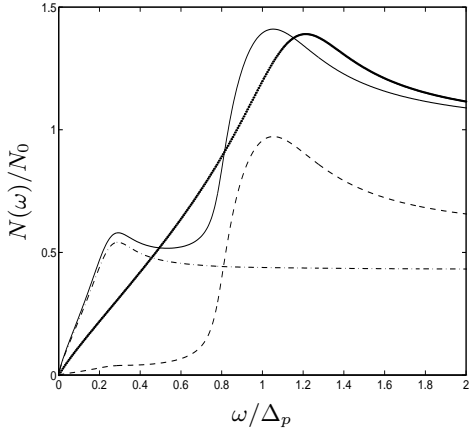


Fig. 4

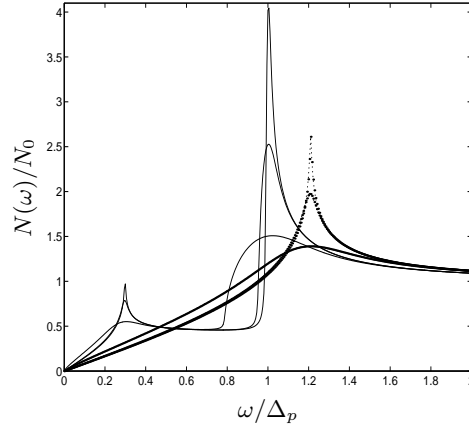


Fig. 5

Fig. 4 – The density of states is shown for medium strength impurities for the multigap model: in the passive band (dashed-dotted line), active band (dashed line) and the full DOS (solid line). The corresponding f-wave DOS (dotted line) exhibits one single peak at  $\omega = 1.21\Delta_p$ .

Fig. 5 – The density of states is shown for the multigap (solid line) and f-wave model (dotted line) for  $U_{11} = U_{22} = U$ ,  $\Gamma = 0.001\Delta_p$ ,  $0.01\Delta_p$  and  $0.1\Delta_p$ ,  $\Gamma_{12}N_0/N_2$  is fixed to  $0.01\Delta_p$ .

as

$$\text{Re}\sigma_l(\omega) = \frac{e^2 n}{2\omega m} \int_0^\omega \text{Re} \left\{ F_l[u_l(\omega - x), -u_l(x)] - F_l[u_l(\omega - x), -\overline{u_l(x)}] \right\} dx, \quad (11)$$

where [24, 25]

$$F_1(u, u') = \frac{2}{\pi\Delta_2} \frac{1}{u' - u} \left( \frac{u'}{\sqrt{1-u'^2}} K\left(\frac{1}{\sqrt{1-u'^2}}\right) - \frac{u}{\sqrt{1-u^2}} K\left(\frac{1}{\sqrt{1-u^2}}\right) \right), \quad (12)$$

$$F_2(u, u') = \frac{1}{\Delta_p} \frac{1}{u' - u} \left( \frac{u'}{\sqrt{1-u'^2}} - \frac{u}{\sqrt{1-u^2}} \right). \quad (13)$$

For the f-wave model, the conductivity reads as

$$\text{Re}\sigma(\omega) = \frac{e^2 n}{2\omega m} \int_0^\omega \text{Re} \left\{ F_1[u(\omega - x), -u(x)] - F_1[u(\omega - x), -\overline{u(x)}] \right\} dx, \quad (14)$$

and  $\Delta_2$  in  $F_1(u, u')$  has to be replaced by  $\Delta_f$ .

From the density of states of the multigap model, one would expect peaks in the conductivity at  $\omega = 2\Delta_2$ ,  $2\Delta_p$ , and if interband scattering is strong enough, at  $\omega = \Delta_p + \Delta_2$ . These features can be seen in figs. 6 and 7. Here the intraband scattering parameter was fixed as  $U_{11} = U_{22}$ ,  $\Gamma_{11}N_0/N_1 = 0.001\Delta_p$  and  $0.01\Delta_p$ , respectively, and the interband scattering parameter varied from weak through medium to strong as  $\Gamma_{21} = 0.1\Gamma_{11}$ ,  $\Gamma_{11}$  and  $10\Gamma_{11}$ . Along this line, as  $\Gamma_{21}$  enhances, the peak corresponding to interband excitations at  $\omega = \Delta_p + \Delta_2$  becomes dominant, overwhelming the intraband processes.

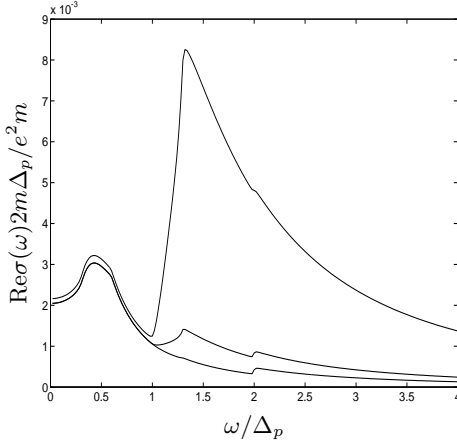


Fig. 6

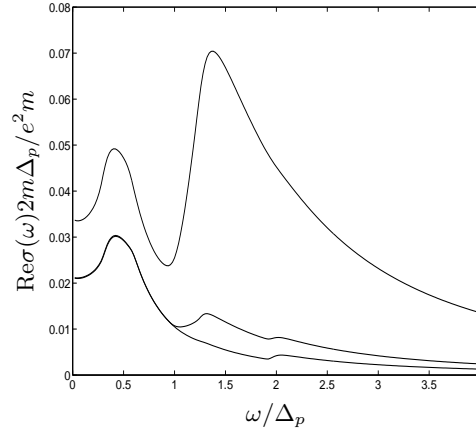


Fig. 7

Fig. 6 – The optical conductivity of the multigap model is plotted for  $U_{11} = U_{22}$ ,  $\Gamma_{11}N_0/N_1 = 0.001\Delta_p$ , the interband scattering parameter changes as  $\Gamma_{21} = 0.1\Gamma_{11}$ ,  $\Gamma_{11}$  and  $10\Gamma_{11}$ , with increasing peak at  $\omega = 1.3\Delta_p$ .

Fig. 7 – The optical conductivity of the multigap model is plotted for  $U_{11} = U_{22}$ ,  $\Gamma_{11}N_0/N_1 = 0.01\Delta_p$ , the interband scattering parameter changes as  $\Gamma_{21} = 0.1\Gamma_{11}$ ,  $\Gamma_{11}$  and  $10\Gamma_{11}$ , with increasing peak at  $\omega = 1.3\Delta_p$ .

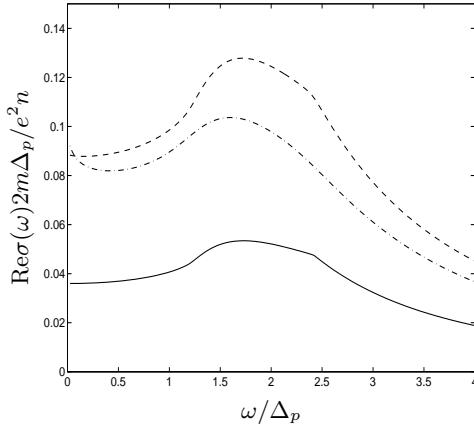


Fig. 8

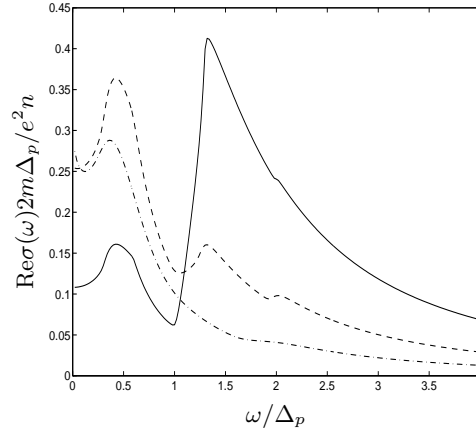


Fig. 9

Fig. 8 – The optical conductivity of the f-wave model is shown for  $\Gamma_{11}N_0/N_1 = 0.001\Delta_p$  (solid line, enlarged by 50),  $0.01\Delta_p$  (dashed line, enlarged by 12) and  $0.1\Delta_p$  (dashed-dotted line).

Fig. 9 – The optical conductivity of the multigap model is shown for  $\Gamma_{12}N_0/N_2 = 0.01\Delta_p$ ,  $\Gamma_{11}N_0/N_1 = 0.001\Delta_p$  (solid line, enlarged by 50),  $0.01\Delta_p$  (dashed line, enlarged by 12) and  $0.1\Delta_p$  (dashed-dotted line).

In the f-wave case, the conductivity is identical to those of a d-wave superconductor, and exhibits a small peak at  $\omega = 0$  as the impurities get stronger, and at the same time a rather

broad bump is developed at  $\omega = 1.5 - 2\Delta_p$  as is seen in fig. 8. It is remarkable also, that in spite of the different scattering rates changing within two orders of magnitude, the curves look rather similar to each other, and can easily be distinguished from the multigap model. For the multigap model, as intraband scattering becomes dominant, the conductivity of the passive band rules over the other transitions, since the same impurities decrease the superfluid density much faster in this band due to the smaller gap (see fig. 9!).

*Conclusion.* – We have calculated the density of states and the optical conductivity for ZR’s multigap model and for the f-wave case in the Born scattering limit. The effect of interband scattering produces new structures in the optical response of the multigap model: resonant peaks can be observed at  $\omega = 2\Delta_2, 2\Delta_p$ , and due to interband transitions at  $\Delta_2 + \Delta_p$ . Therefore when the experimental difficulty to perform the optical measurement below  $T = 0.1\text{K}$  is overcome, this will provide a unique way to explore the validity of models for the superconductivity in  $\text{Sr}_2\text{RuO}_4$ . In a forthcoming paper we shall discuss the effect of resonant scatterers, where we also expect clear differences between the multigap and f-wave model.

*Acknowledgments.* – We are benefited from useful discussions with Hyekyung Won and Peter Thalmeier. This work was supported by the Hungarian National Research Fund under grant numbers OTKA T032162 and T037451.

## REFERENCES

- [1] Y. Maeno, H. Hashimoto, K. Yoshida, S. Nishizaki, T. Fujita, J. G. Bednorz, and F. Lichtenberg, *Nature (London)* **372**, 532 (1994).
- [2] T. M. Rice and M. Sigrist, *J. Phys. Cond. Mat.* **7**, L643 (1995).
- [3] Y. Maeno, T. M. Rice, and M. Sigrist, *Physics Today* **54**, 42 (2001).
- [4] G. M. Luke *et al.*, *Nature (London)* **394**, 558 (1998).
- [5] K. Ishida *et al.*, *Phys. Rev. Lett.* **84**, 5387 (2000).
- [6] S. Nishizaki, *J. Phys. Soc. Jpn* **67**, 560 (1998).
- [7] E. Puchkaryov and K. Maki, *Europhys. Lett.* **45**, 263 (1999).
- [8] S. Nishizaki *et al.*, *J. Phys. Soc. Jpn* **69**, 572 (2000).
- [9] I. Bonalde *et al.*, *Phys. Rev. Lett.* **85**, 4775 (2000).
- [10] K. Ishida *et al.*, *Nature (London)* **396**, 658 (1998).
- [11] M. Tanatar *et al.*, *Phys. Rev. Lett.* **86**, 2649 (2001).
- [12] M. Tanatar *et al.*, *Phys. Rev. B* **63**, 064505 (2001).
- [13] C. Lupien *et al.*, *Phys. Rev. Lett.* **86**, 5986 (2001).
- [14] K. Miyake and O. Narikiyo, *Phys. Rev. Lett.* **83**, 1423 (1999).
- [15] M. J. Graf and A. V. Balatsky, *Phys. Rev. B* **62**, 9697 (2000).
- [16] T. Dahm, H. Won, and K. Maki, *cond-mat/0006301*.
- [17] K. Izawa *et al.*, *Phys. Rev. Lett.* **86**, 2653 (2001).
- [18] H. Won and K. Maki, *Physica B* **312-313**, 44 (2002).
- [19] M. E. Zhitomirsky and T. M. Rice, *Phys. Rev. Lett.* **87**, 057001 (2001).
- [20] H. Won and K. Maki, *Phys. Rev. B* **49**, 1397 (1994).
- [21] H. Kusunose and M. Sigrist, *Europhys. Lett.* **60**, 281 (2002).
- [22] D. F. Agterberg, *Phys. Rev. B* **60**, R749 (1999).
- [23] A. P. Mackenzie, S. R. Julian, A. J. Diver, G. J. McMullan, M. P. Ray, G. G. Lonzarich, Y. Maeno, S. Nishizaki, and T. Fujita, *Phys. Rev. Lett.* **76**, 3786 (1996).
- [24] B. Dóra, A. Virosztek, and K. Maki, *Physica C* **341-348**, 775 (2000).
- [25] B. Dóra, K. Maki, and A. Virosztek, *cond-mat/0012198*.